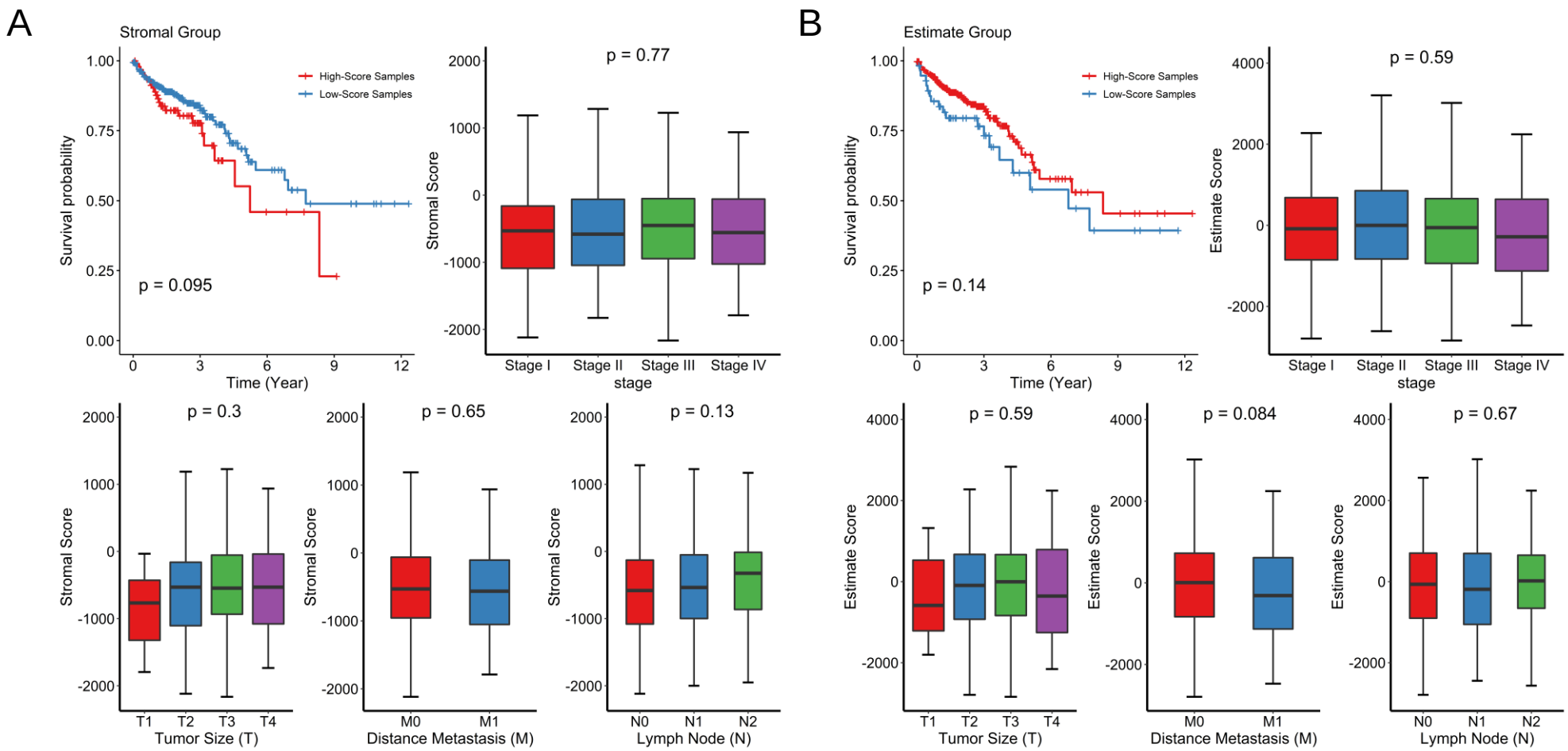

Figure S1 The comparisons of the distributions of (A) stromal scores and (B) estimate scores on TNM stage, tumor size, distant metastasis, lymph nodes and overall survival time.

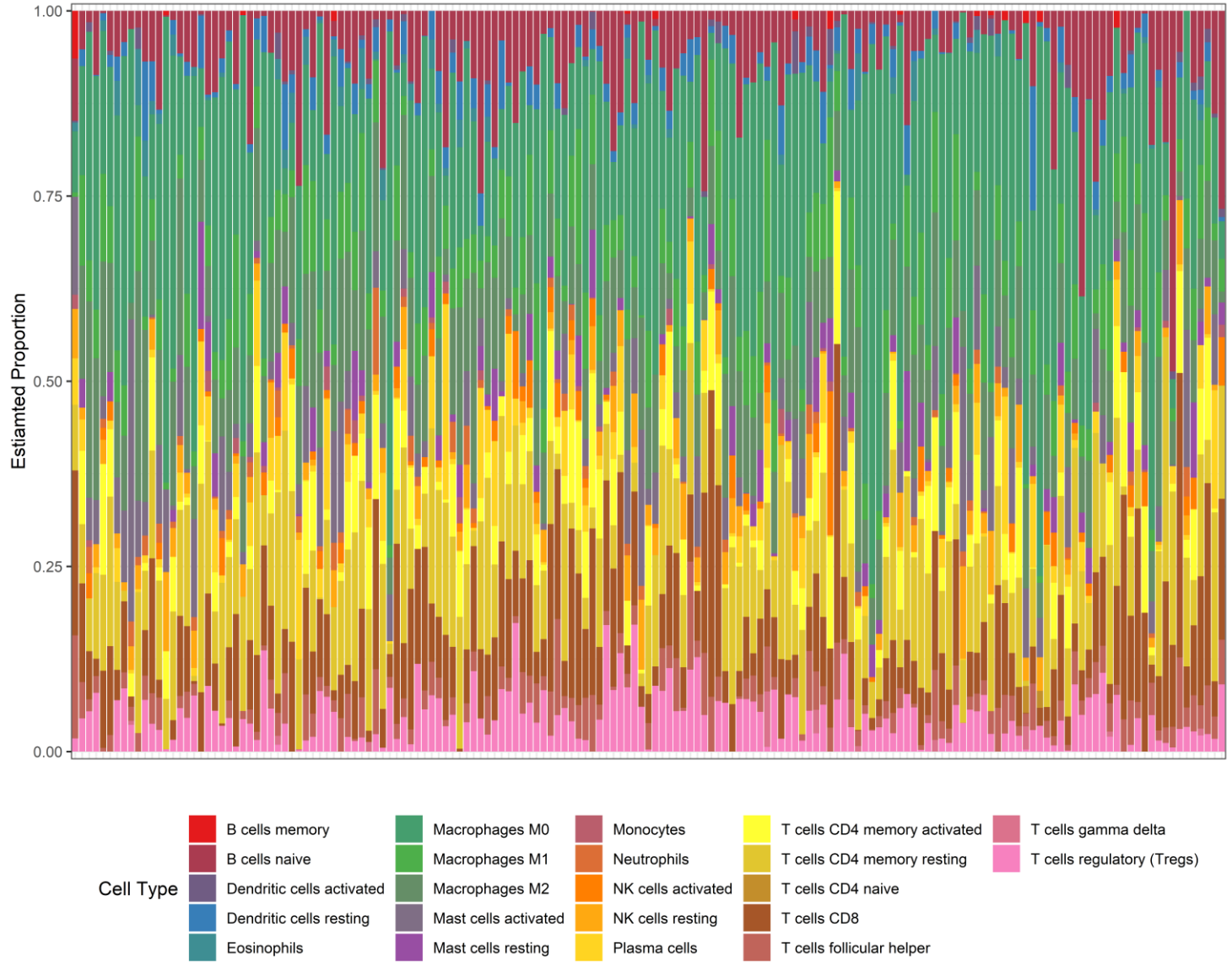

Figure S2 The immune infiltrating cell composition of each sample with a CIBERSORT' P value less than 0.05

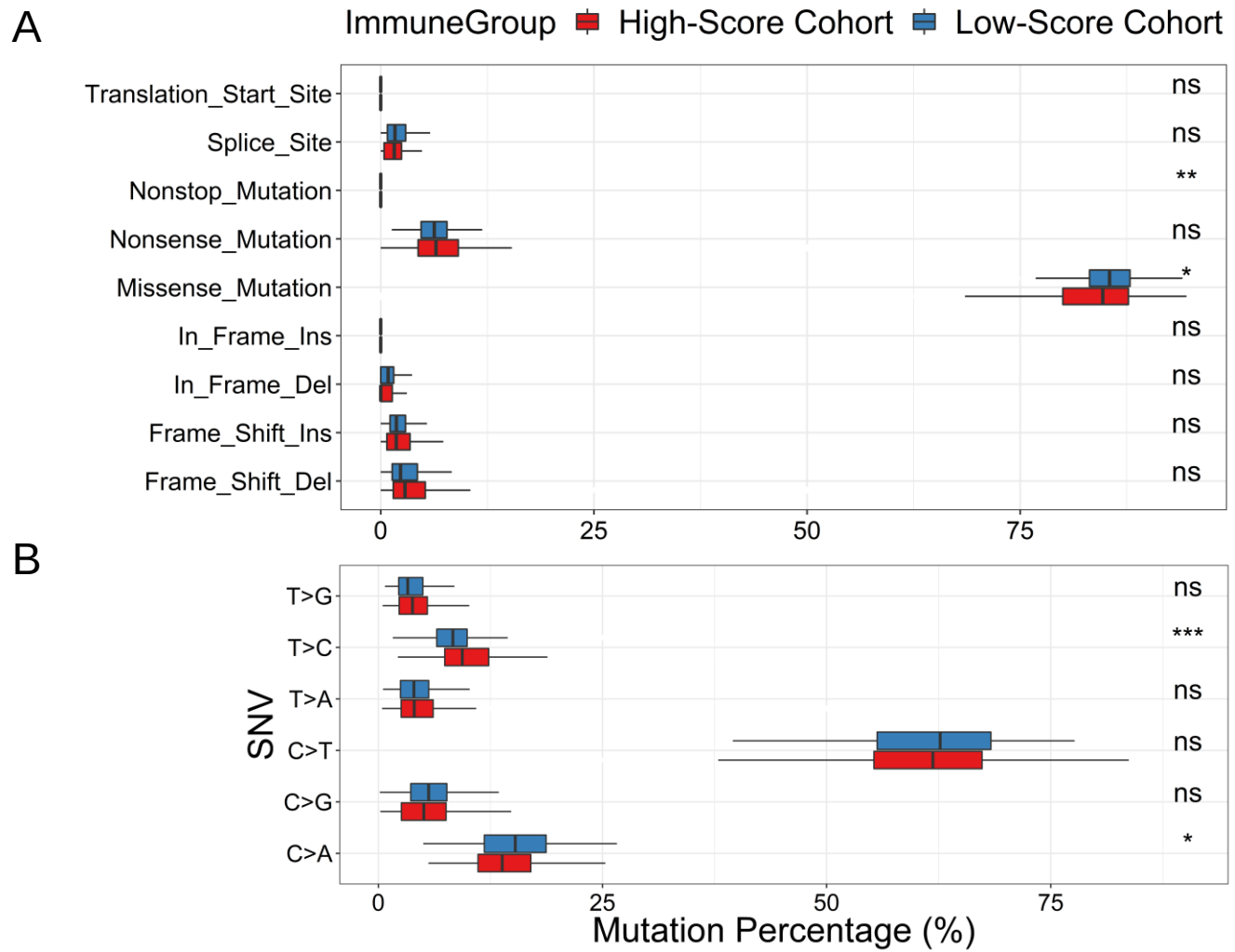

Figure S3 The percentages of various mutation types in high-immunity and low-immunity cohorts. Boxplots respectively display the comparisons of the percentages of (A) every mutation type classified by effects, (B) SNV. Symbols indicated statistical significance for the wilcox test: ns, $P > 0.05$; *, $P \leq 0.05$; **, $P \leq 0.01$; ***, $P \leq 0.001$.

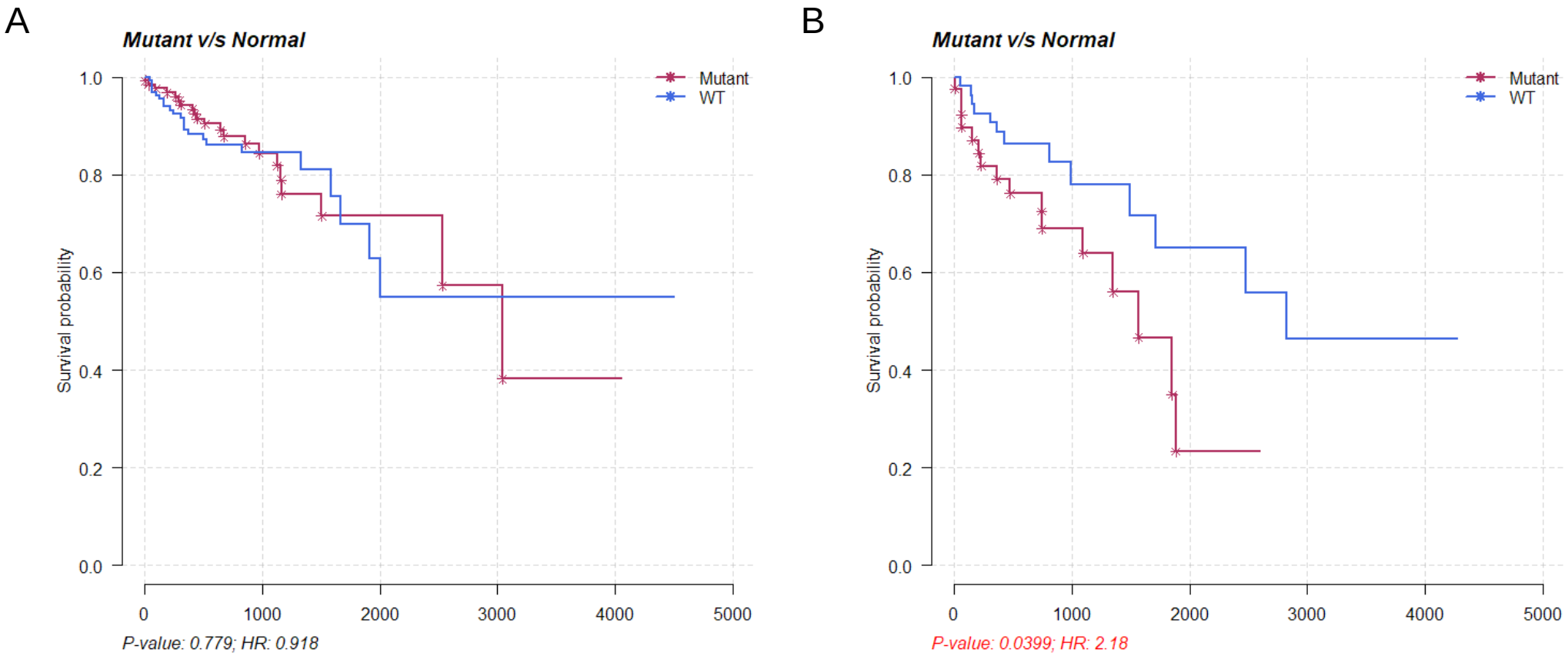

Figure S4 Kaplan-Meier curves show the independent relevance between overall survival time and TTN mutation in (A) high-immunity group(B) low-immunity group.

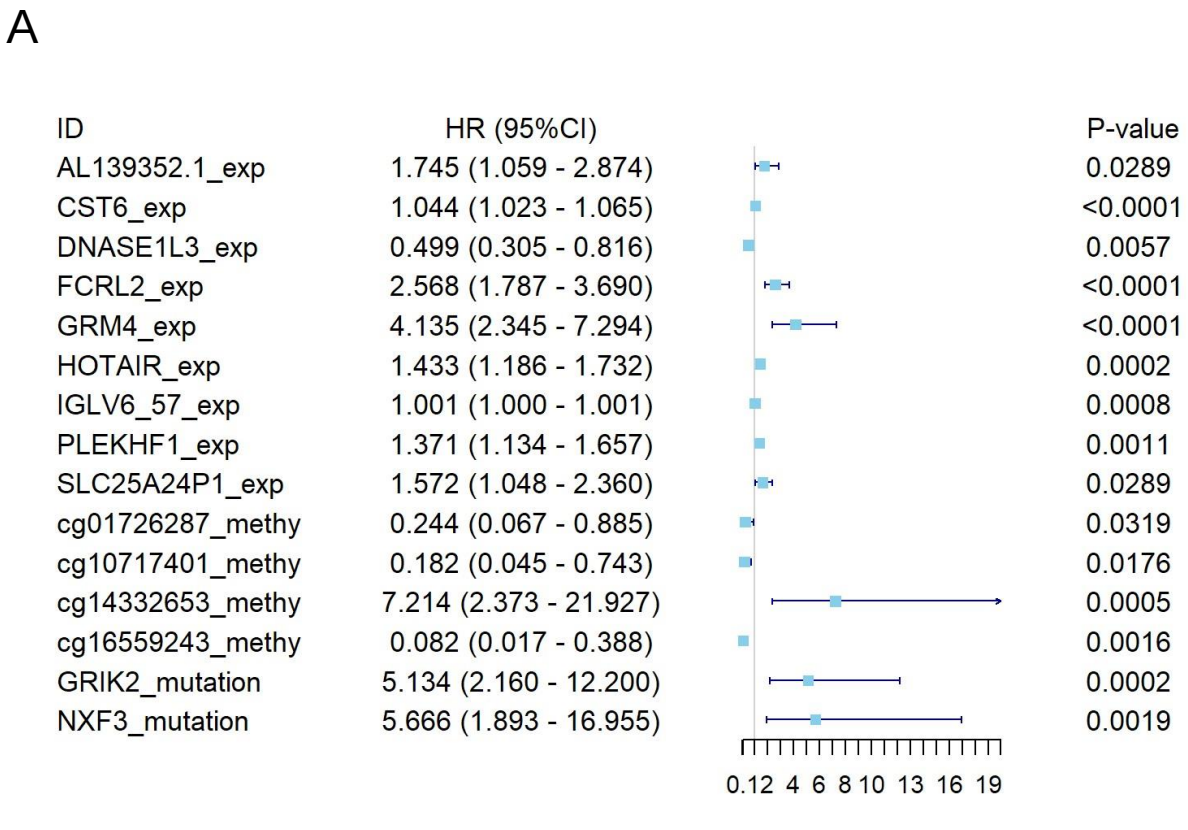

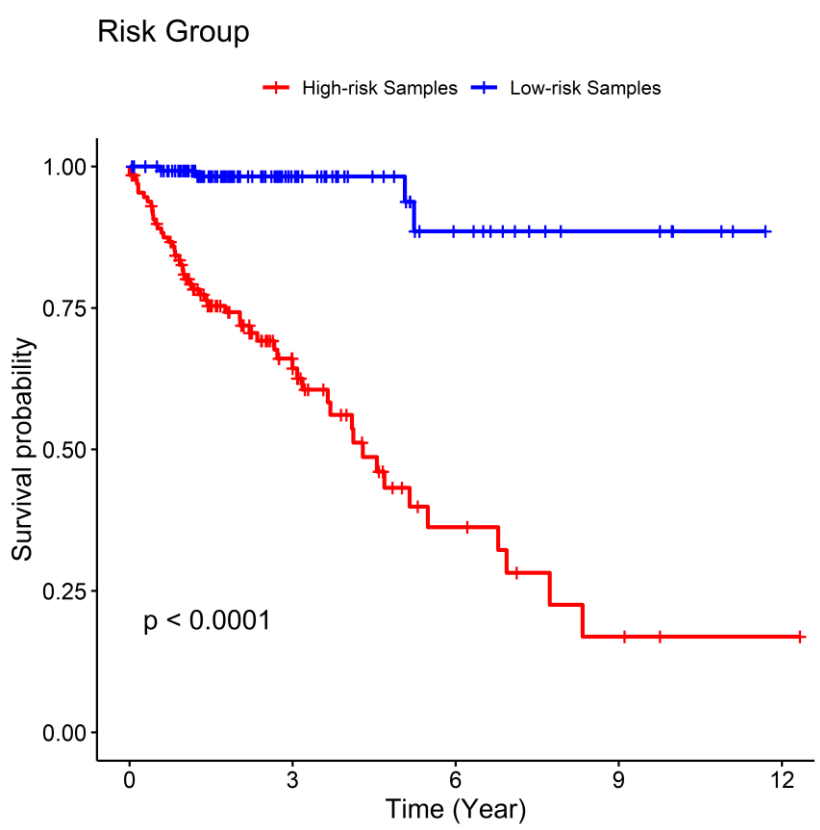

Figure S5 (A) Forest plot of the prognostic impact of genetic and epigenetic variables. (B) Kaplan-Meier curves show the independent relevance between overall survival time and risk scores.

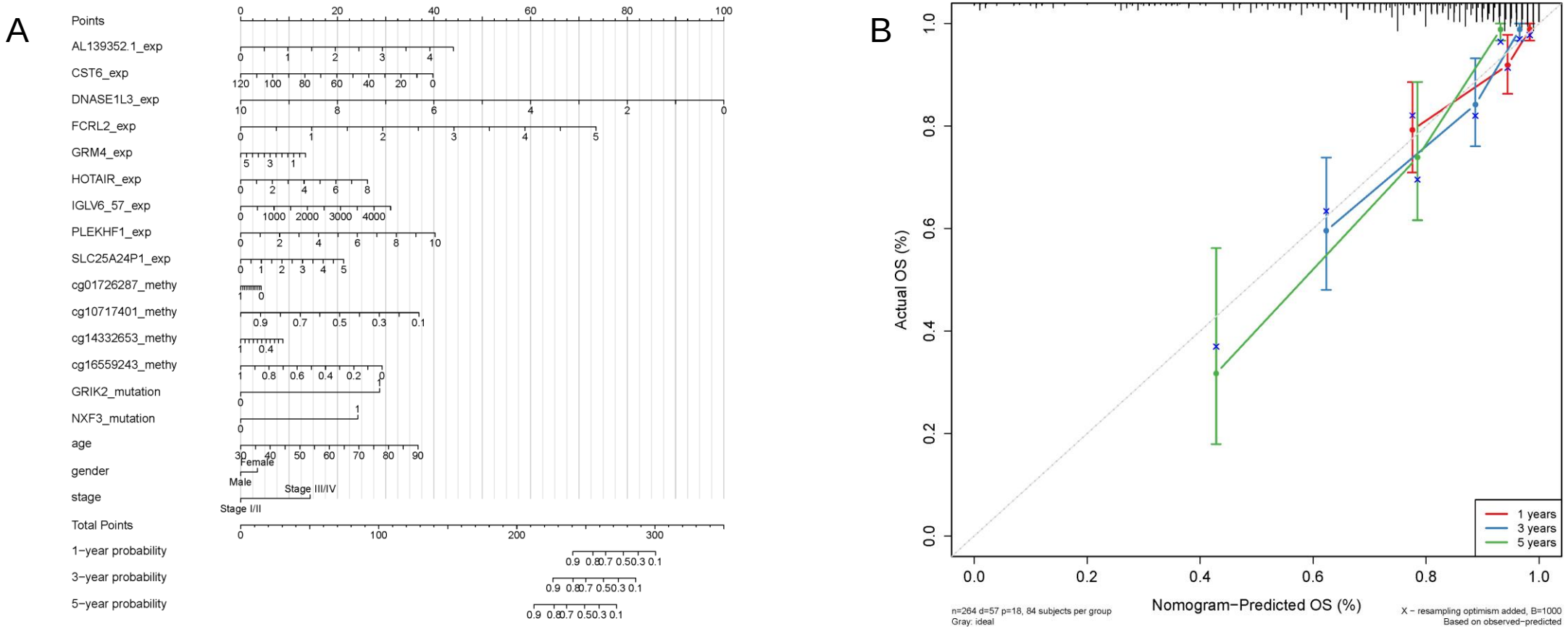

Figure S6 Nomogram (A) and calibration plot (B) for prediction of overall survival time based on the combination of multi-omics characteristics and clinical factors in CRC.

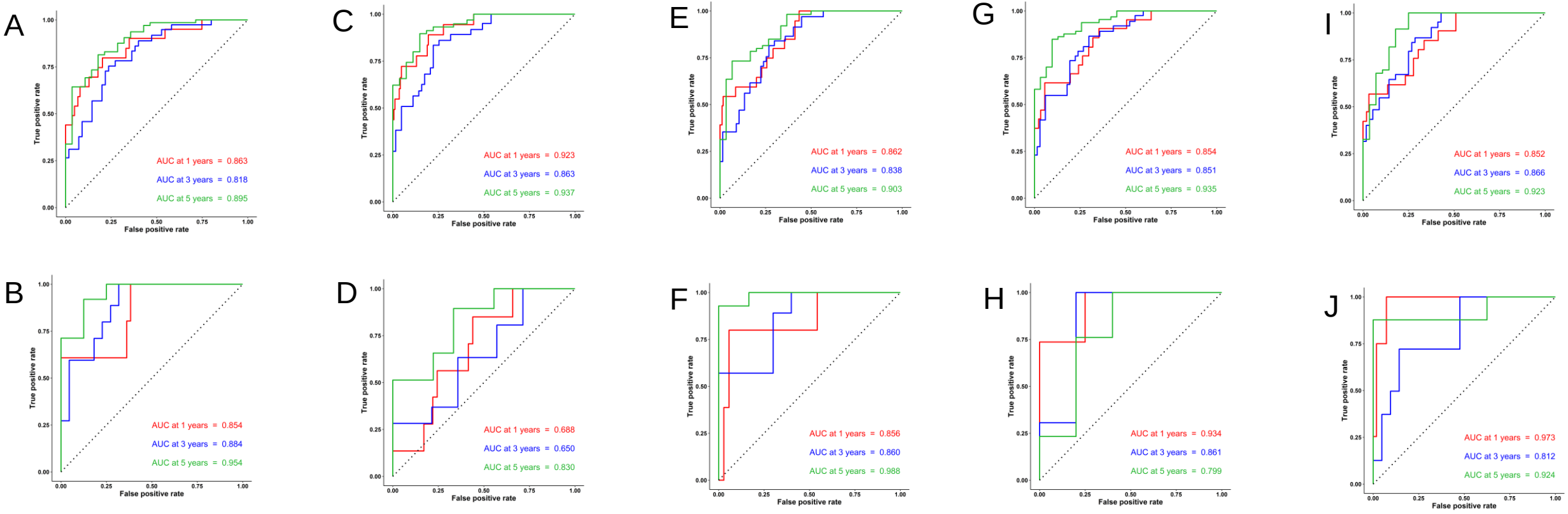

Figure S7 The performance of the 5-fold cross validation set 1 (A-B), set 2 (C-D), set 3 (E-F), set 4 (G-H) and set 5 (I-J). Subplot (A/C/E/G/I) and (B/D/F/H/J) show the roc curves of the risk score for 1-year, 3-year and 5-year survival prediction on the training set and test set, respectively.